

## Fibrin-Targeting, Peptide Amphiphile Micelles as Contrast Agents for Molecular MRI

Eun Ji Chung<sup>1</sup>, Federico Pineda<sup>2</sup>, Kathryn Nord<sup>1</sup>, Gregory Karczmar<sup>2</sup>, Seon-Kyu Lee<sup>2</sup> and Matthew Tirrell<sup>1\*</sup>

<sup>1</sup>Institute for Molecular Engineering, University of Chicago, 5747 S. Ellis Ave., Chicago, IL, 60637, USA

<sup>2</sup>Department of Radiology, University of Chicago, 5841 S. Maryland Ave., MC2026, Chicago, IL 60637, USA

### Abstract

Magnetic resonance imaging (MRI) provides a nonionizing and safe imaging modality for cancer diagnostics. Here, we took advantage of the fibrin deposition that is characteristic of tumors and the ability to incorporate multiple functionalities within peptide amphiphile micelles (PAMs) to design a new class of contrast agents for molecular MRI. We report on synthesis, formulation, and preliminary tests for MRI of spherical PAMs that were self-assembled by combining 18:0 PE-DTPA (Gd) and peptide amphiphiles containing the fibrin-binding pentapeptide, cysteine-arginine-glutamic acid-lysine-alanine, or CREKA. Conjugation of the CREKA peptide to micelles increased the average particle size and zeta potential, and T1 relaxivities of CREKA-Gd PAMs (per mmol of Gd) were found to be comparable to contrast agents which are used routinely in clinical settings at 1.5T and 3T. Moreover, when murine fibroblasts were cultured with CREKA-Gd PAMs, no cytotoxicity was demonstrated and cell viability was comparable to that of PBS-treated controls for up to 3 days. Our study provides proof-of-concept of CREKA-Gd PAMs as contrast agents for molecular MRI, and a facile strategy for incorporating contrast agents and bioactive molecules into nano carriers to develop safe, targeted diagnostic carriers for clinical application.

**Keywords:** Micelle; Targeting; Peptide; Magnetic Resonance Imaging (MRI); Fibrin; Self-assembly

### Introduction

Magnetic resonance imaging (MRI) is a preferred diagnostic imaging modality of cancer evaluation because it is noninvasive, does not use ionizing radiation, and provides strong soft tissue contrast [1]. Nanocarriers can be combined with complexes of paramagnetic compounds such as gadolinium (III) (Gd) to passively target tumor tissue and deliver Gd through the enhanced permeability and retention (EPR) effect [2-4]. However, the inherent low relaxivity and low specificity to tissues limit applications of this approach [5].

Our group has successfully developed a fluorescently-labeled, fibrin-binding peptide amphiphile micelle (PAM) for cancer targeting using the pentapeptide, cysteine-arginine-glutamic acid-lysine-alanine (CREKA) [4,6,7]. Fibrin-targeting is an effective strategy for selectively enhancing cancers because tumors, but not normal tissues, have leaky, hemorrhagic vasculature, which contributes to thrombosis and fibrin deposition [8,9]. PAMs are advantageous as therapeutic and/or diagnostic carriers because a concentrated, multivalent display of a peptide can produce efficient binding to a molecular, tumor target of interest [5,10]. Moreover, the nanometer size of PAMs including a poly(ethylene glycol) (PEG) protective shell provides favorable pharmacokinetic properties *in vivo* and can prolong bioavailability and deliver drugs and contrast agents in the optimum dosage range, which results in reduced, toxic side effects [11].

In order to integrate the molecular targeting capabilities of PAMs and the diagnostic performance of MRI, we combined peptide amphiphiles (PA) consisting of the CREKA peptide and 18:0 PE-DTPA (Gd) to self-assemble micelles that can be utilized as molecular MRI contrast agents for tumor-targeting. Unlike other nanoparticle systems in which Gd is covalently incorporated into the structures of nanocarriers, increasing the risk of Gd<sup>3+</sup> ion leakage from the chelates due to the prolonged half-life in the body and cumulative toxicity [12], our micelles were designed such that tumor-targeting, imaging, and release of 18:0 PE-DTPA (Gd) can be easily achieved. In this study,

we assessed the potential of these novel CREKA-Gd PAMs as contrast agents for MRI applications and evaluated biocompatibility *in vitro*.

### Materials and Methods

#### CREKA-Gd PAM synthesis and construction

The [Cys-Arg-Glu-Lys-Ala] peptide was synthesized using standard Fmoc-mediated solid phase peptide synthesis methods on Rink amide resin (Anaspec, Fremont, CA, USA) using an automated PS3 Benchtop Peptide Synthesizer (Protein Technologies, Tucson, AZ, USA) as previously described [4]. Peptides were cleaved and deprotected with 94:2.5:2.5:1 by volume trifluoroacetic acid:1,2-ethanedithiol:H<sub>2</sub>O:triisopropylsilane and were precipitated and washed several times with cold diethyl ether, dissolved in water, lyophilized, and stored as lyophilized powders at 20°C. Crude, peptide mixtures were purified by reverse-phase HPLC (Prominence, Shimadzu, Columbia, MD, USA) on a C8 column (Waters, Milford, MA) at 55°C using 0.1% trifluoroacetic acid in acetonitrile/water mixtures and characterized by MALDI-TOF/TOF mass spectral analysis (Biflex III, Bruker, Billerica, MA, USA). Cysteine-containing peptides were conjugated via a thioether linkage to DSPE-PEG (2000)-maleimide (Avanti Polar Lipids, Alabaster, AL, USA) by adding a 10% molar excess of the lipid to peptide in water. After reaction at RT for 24 hours, the resulting product was purified and characterized as described above.

\*Corresponding author: Matthew Tirrell, Institute for Molecular Engineering, University of Chicago 5747 S. Ellis Ave., Chicago, IL, 60637, USA, Tel: +1-773-834-2023; Fax: +1-773-834-7756; E-mail: [mtirrell@uchicago.edu](mailto:mtirrell@uchicago.edu)

Received: July 12, 2014; Accepted: September 26, 2014; Published: September 29, 2014

Citation: Chung E, Pineda F, Nord K, Karczmar, Lee SK, et al. (2014) Fibrin-Targeting, Peptide Amphiphile Micelles as Contrast Agents for Molecular MRI. J Cell Sci Ther 5: 181. doi:10.4172/2157-7013.1000181

Copyright: © 2014 Chung E, et al. This is an open-access article distributed under the terms of the Creative Commons Attribution License, which permits unrestricted use, distribution, and reproduction in any medium, provided the original author and source are credited.

CREKA-Gd PAMs were assembled by dissolving DSPE-PEG (2000)-CREKA amphiphiles and 18:0 PE-DTPA (Gd) (Avanti Polar Lipids, Alabaster, AL, USA) in chloroform (75:25 molar ratio, unless otherwise stated), mixing the components, and evaporating the mixed solution under nitrogen gas. The resulting film was dried under vacuum O/N, and then hydrated at 80°C for 30 minutes in PBS under sonication, and allowed to cool to RT. Non-targeting, control-Gd PAMs were self-assembled by combining 18:0 PE-DTPA (Gd) and DSPE-PEG(2000)-maleimide.

### Transmission Electron Microscopy (TEM)

Samples for TEM were prepared by placing the 100 µM CREKA-Gd or control-Gd PAM solution on 400 mesh lacey carbon grids (Ted Pella, Redding, CA, USA) for 2 minutes. Excess liquid was wicked away with filter paper and the grid was washed with Milli-Q water. Dried samples were imaged on a JEOL 1230 TEM, immediately (JEOL, Ltd., Tokyo, Japan).

### Dynamic Light Scattering (DLS)

Stock solutions of 100 µM CREKA-Gd or control-Gd PAMs were used to confirm the presence of small spheroidal micelles and DLS measurements were determined at 90° and 637 nm using a Brookhaven Instruments (Holtzville, NY, USA) system consisting of a BI-200SM goniometer and a BI-9000AT autocorrelator (N=3).

### Zeta potential

Zeta potential of 100 µM CREKA-Gd or control-Gd PAMs were measured (Zetasizer Nano ZS, Malvern, Worcestershire, United Kingdom, N=3).

### MRI acquisitions

Relaxivity of the CREKA-Gd PAMs were measured at both 1.5T and 3T, on Philips Achieva scanners (Philips Healthcare, Best, The Netherlands), using surface coils. The T1's (longitudinal relaxation times) of vials containing CREKA-Gd PAMs with varying concentrations of Gd (0 mM, 0.1 mM, 0.25 mM, 0.5 mM) were measured. The T1-mapping sequence consisted of a fast spin echo inversion recovery (FSE-IR) with varying inversion times. The FSE-IR acquisition parameters were as follows: TR = 12 s; TE = 15 ms; TI (inversion times) = 50, 100, 250, 500, 750, 1000, 2000, 3000, 4000, 5000 ms; acquisition voxel size of 1 mm × 1 mm and 3 mm slice thickness. Data analysis was performed off-line with in-house software written in Matlab (MathWorks, Natick, MA, USA). The FSE-IR images were fit, using a nonlinear least squares fitting algorithm, on a voxel-by-voxel basis to the signal model (Equation 1):

$$M(TI) = M_0 \left( 1 - 2e^{-\frac{TI}{T1}} + e^{-\frac{TR}{T1}} \right)$$

Where M (TI) is the measured signal at each inversion time (TI) and M<sub>0</sub> is the equilibrium magnetization. These fits yielded a T1 value for each voxel. The mean T1 for each sample, and thus each concentration of Gd, was measured by drawing regions of interest in all the vials, which had a cross sectional diameter of 9 mm in the acquisition plane.

In the fast exchange limit, the longitudinal relaxation rates have a linear relationship with contrast concentration, where the relaxivity of the contrast media (r<sub>1</sub>) is the slope of the curve (Equation 2):

$$\frac{1}{T1(C)} - \frac{1}{T1,0} = r_1 C$$

where T1,0 is the native T1 (in the absence of any contrast media) and C is the concentration. The T1 values measured from the FSE-

IR data at both 1.5T and 3T were fit to Equation 2 to determine the relaxivity at each field strength.

The T1 and T2 relaxation times of the control-Gd and CREKA-Gd PAMs were measured at 1.5T. A FSE-IR sequence, with the same acquisition parameters as described above, was acquired to measure T1. The T2's were measured with a spin echo (SE) sequence with varying echo times (TEs). The SE were acquired with the following acquisition parameters: TR = 100 ms; TE's = 8, 10, 15, 20, 30, 40, 50 ms; acquisition voxel size of 1 mm × 1 mm and 3 mm slice thickness. FSE-IR data were fit to Equation 1 to determine the T2. The SE data were fit to the spin echo signal model to obtain estimates of T2 (Equation 3):

$$M(TE) = M_0 \left( 1 - e^{-\frac{TR}{T1}} \right) e^{-\frac{TE}{T2}}$$

The mean T1 and T2 values of control-Gd and CREKA-Gd PAMs were calculated by drawing ROIs over the vials in the calculated T1 and T2 maps.

### Cell culture

The murine fibroblast cell line NIH/3T3 was purchased from ATCC (Manassas, VA, USA) and cultured and expanded in Dulbecco's Modified Eagle's Medium supplemented with 10% fetal bovine serum and 1% penicillin/streptomycin. Cells were cultured at 37°C in a humidified incubator under 5% CO<sub>2</sub>. Cells at passage 3 were used and media was changed every 2-3 days.

### In vitro biocompatibility

To assess biocompatibility, 10,000 fibroblasts were cultured within 96-well plates and after 24 hr, 20 µL of PBS or 1 mM CREKA-Gd or control-Gd PAMs were added to 180 µL of growth media (100 µM final PAM concentration). After 1 or 3 days of incubation, cell viability was determined by a Live/Dead assay kit (Molecular Probes, Eugene, OR, USA) and Presto Blue assay (Life Technologies, Grand Island, NY, USA N≥3). Cells were imaged on a Leica DMI6000B fluorescence microscope at 4x magnification (Buffalo Grove, IL, USA).

### Statistical analysis

Data are expressed as mean ± SEM. A Student's t-test was used to compare means of pairs and analysis of variance (ANOVA) using Tukey multiple comparison test post-hoc analysis to determine significant differences among three or more means. A p-value of 0.05 or less was considered to be significant.

### Results and Discussion

The non-targeting, control amphiphile, DSPE-PEG (2000)-maleimide, or the fibrin-binding PA, DSPE-PEG (2000)-CREKA, was combined with 18:0 PE-DTPA (Gd) in a 75:25 molar ratio and the presence of spherical micelles with an average diameter 9.3 ± 1.2 and 12.4 ± 1.4 nm was confirmed via TEM and DLS (Figure 1 and Table 2). Zeta potentials of CREKA-Gd and control-Gd PAMs were determined to be -10.5 ± 0.1 and -24.1 ± 0.1 mV, respectively (Table 1). The conjugation of the peptide, CREKA, to DSPE-PEG(2000)-maleimide slightly increased the micelle size and zeta potential, which is consistent with our previous studies [4]. The surface charge of control-Gd PAMs can be attributed to the phosphate group of the DSPE tail, PEG molecules, and the maleimide, which is increased by the addition of the arginine and lysine-containing peptide. For control-Gd PAMs (1 mM) consisting of 25 mol. % 18:0 PE-DTPA (Gd), T1 and T2 measurements were determined to be 330.0 ± 3.3 and 72.0 ± 3.6 ms (Table 1). T1 and T2 values of control-Gd PAMs

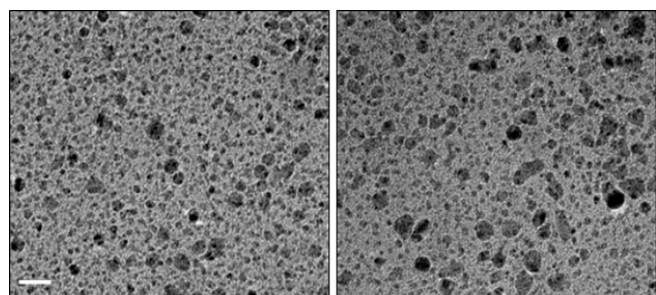


**Figure 1:** Transmission electron micrographs of A) control-Gd and B) CREKA-Gd PAMs show spherical shaped micelle combined Gadolinium. SB: 20 nm. Arrows point to PAMs.

	Control-Gd	CREKA-Gd
Size (nm)	9.3 ± 1.2	12.4 ± 1.4
ZP (mV)	-24.1 ± 0.1	-10.5 ± 0.1
T1 (ms)	330.0 ± 3.3	399.0 ± 4.5
T2 (ms)	72.0 ± 3.6	92.0 ± 4.5

**Table 1:** Characterization of control-Gd and CREKA-Gd PAMs.

with the same Gd content increased to 399.0 ± 4.5 and 92.0 ± 4.5 ms, respectively. T1 and T2 values for micelles with no Gd are 2726.8 ± 7.5 and 95.0 ± 10.6 ms, respectively.

When the Gd content was changed within CREKA PAMs and micelles were constructed with varying 18:0 PE-DTPA (Gd) to DSPE-PEG (2000)-CREKA ratios, an increase in Gd led to a decrease in T1 measurements via both 1.5T and 3T as expected [13], confirming the modularity of PAMs as contrast agents for MRI (Table 2). T1 relaxation times upon incorporation of 50 mol. % Gd into micelles were 183.4 ± 0.9 ms and 223.1 ± 1.54 ms at 1.5T and 3T, respectively, which increased to 381.3 ± 2.2 ms and 434.2 ± 5.3 ms with 25 mol. % Gd, and 890.9 ± 2.2 ms and 970.0 ± 3.0 ms with 10 mol. % Gd. Without any Gd, T1 measurements of micelles were similar to that of water (2.7 s) [14]. Furthermore, Figure 2 shows that the T<sub>1</sub> relaxivity (r<sub>1</sub>) of CREKA-Gd was 9.87 mM<sup>-1</sup>s<sup>-1</sup> at 1.5T and 8.08 mM<sup>-1</sup>s<sup>-1</sup> at 3T (where the units are in millimoles of Gd). These relaxivities are higher than those of several contrast agents used routinely in clinical settings [15], suggesting that areas with higher uptake of CREKA-Gd will be easily visualized in T1-weighted images *in vivo*. This may be explained by enhanced rotational correlation times and spectral density characteristic to Gd<sup>3+</sup> complexed with macromolecules such as polymers or proteins [16]. Moreover, our results are consistent with other groups who report nanoparticles with Gd<sup>3+</sup> bound to PE-DTPA to show a strong paramagnetic relaxation effect on surrounding water protons [17]. Interestingly, micelles consisting entirely of 18:0 PE-DTPA (Gd) had relaxation times of 386.6 ± 2.72 ms and 465.8 ± 2.54 ms at 1.5T and 3T, respectively (data not shown). This phenomenon is likely to result from the proximity of paramagnetic ions to one another within micelles as reported for liposome systems consisting of PE-DTPA (Gd), as well as for the relaxivity of Mn<sup>2+</sup> ions bound to phosphatidyl serine sonicated vesicles [17,18]. Thus the Gd complex appears most efficient as a contrast agent when present at lower local concentrations in micelles.

Combining gadolinium with CREKA-PAM has the potential to alter surface characteristics of CREKA-PAM complex, and this could change molecular targeting capabilities of PAM especially in *in-vivo* circumstances. However, when fluorescence imaging agents were combined with CREKA-PAMs previously, no change in targeting capabilities was found [4,7]. Moreover, combining other MRI contrast

agents superparamagneticnanonets) with polymeric micelles did not change the targeting capability either [19,20]. Therefore, we believe that CREKA-PAMs combined with gadolinium is likely to maintain its targeting capability. However, future *in vivo* studies specifically assessing the maintenance of the targeting capability of our CREKA-Gd PAM complex as well as possible interactions between combined PAMs and blood will be necessary.

In order to confirm the potential of CREKA-Gd PAMs as safe contrast agents for future MRI applications *in vivo*, cell biocompatibility and viability were assessed using NIH/3T3 fibroblasts *in vitro*. Live/Dead assays confirmed fibroblasts cultured with 100 μM control-Gd or CREKA-Gd for 1 or 3 days were viable with few-to-no dead cells, and were comparable to PBS-treated controls (Figure 3). Moreover, Presto Blue assays further verified cell viability upon treatment with CREKA-Gd PAMs for up to 3 days (Figure 4).

In summary, the fibrin-binding peptide amphiphile was combined with 18:0 PE-DTPA (Gd) to construct CREKA-Gd PAMs as contrast agents for potential MRI applications. Our micelles provide a multifunctional platform that can be easily tailored to incorporate contrast agents such as Gd, targeting peptides, and therapeutics for

Gd:CREKA	1.5T (ms)	3T (ms)
50:50	183.4 ± 0.9	223.1 ± 1.54
25:75	381.3 ± 2.2	434.2 ± 5.3
10:90	890.9 ± 2.2	970.0 ± 3.0
0:100	2726.8 ± 7.5	2714.3 ± 29.2

**Table 2:** T1 measurements of CREKA-Gd PAMs with varying Gd content show with increasing Gd, T1 values decrease confirming potential of micelles as MRI contrast agents.

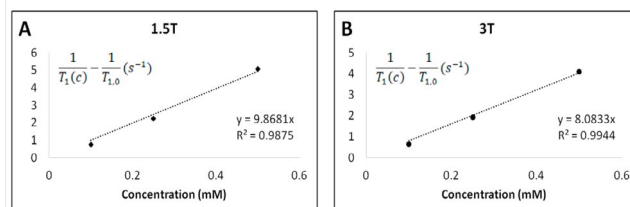


**Figure 2:** Change in relaxation rates Δ(1/T1) vs. concentration of CREKA-Gd PAMs in both 1.5T (A) and 3.0T (B) magnets demonstrates linear correlation.

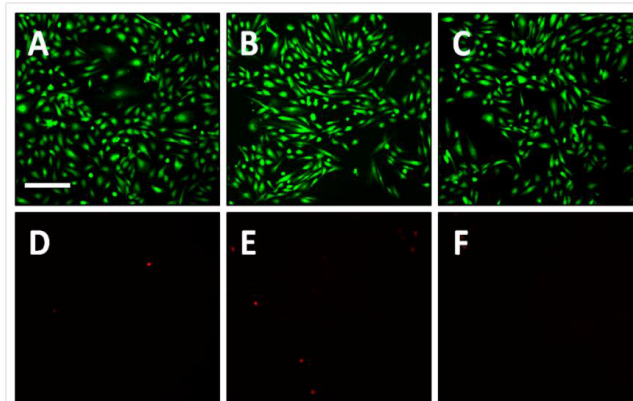
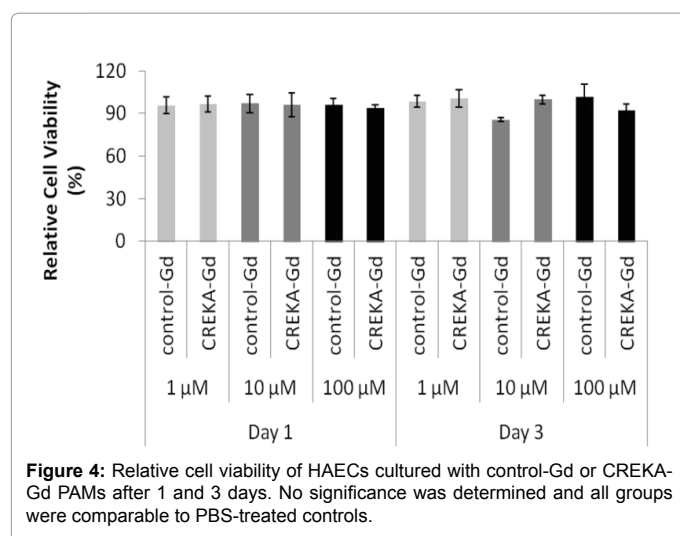


**Figure 3:** Representative live-dead images of HAECs cultured with A/D) control-Gd PAMs, B/E) CREKA-Gd PAMs, and C/F) PBS at day 3 confirm viability. SB: 200 μm.



potential theranostic applications. Future *in vivo* studies within a tumor model will provide the full extent of our novel micelles as safe and potent nanocarriers that can be utilized to detect, image, and treat tumors.

#### Acknowledgement

The authors made use of the equipment and acknowledge assistance from the Mass Spectroscopy Facility, the NSF Materials Research Science and Engineering Center (MRSEC), and the Brain Research Imaging Center (BRIC) at the University of Chicago. This work was supported by an American Heart Association Postdoctoral Fellowship granted to E.J. Chung. There are no conflicts of interests.

#### References

- Mi P, Cabral H, Kokuryo D, Rafi M, Terada Y, et al. (2013) Gd-DTPA-loaded polymer-metal complex micelles with high relaxivity for MR cancer imaging. *Biomaterials* 34: 492-500.
- Kataoka K, Harada A, Nagasaki Y (2001) Block copolymer micelles for drug delivery: design, characterization and biological significance. *Adv Drug Deliv Rev* 47: 113-131.
- Cabral H, Nishiyama N, Kataoka K (2011) Supramolecular nanodevices: from design validation to theranostic nanomedicine. *Acc Chem Res* 44: 999-1008.
- Chung EJ, Cheng Y, Morshed R, Nord K, Han Y, et al. (2014) Fibrin-binding, peptide amphiphile micelles for targeting glioblastoma. *Biomaterials* 35: 1249-1256.
- Trent A, Marullo R, Lin B, Black M, Tirrell M (2011) Structural properties of soluble peptide amphiphile micelles. *Soft Matter* 7: 9572-9582.
- Simberg D, Duza T, Park JH, Essler M, Pilch J, et al. (2007) Biomimetic amplification of nanoparticle homing to tumors. *Proc Natl Acad Sci U S A* 104: 932-936.
- Peters D, Kastantin M, Kotamraju VR, Karmali PP, Gujratty K, et al. (2009) Targeting atherosclerosis by using modular, multifunctional micelles. *Proc Natl Acad Sci U S A* 106: 9815-9819.
- Dvorak HF (2003) Rous-Whipple Award Lecture. How tumors make bad blood vessels and stroma. *Am J Pathol* 162: 1747-1757.
- Dvorak HF, Senger DR, Dvorak AM, Harvey VS, McDonagh J (1985) Regulation of extravascular coagulation by microvascular permeability. *Science* 227: 1059-1061.
- Hamley IW (2011) Self-assembly of amphiphilic peptides. *Soft Matter* 7: 4122-4138.
- Bisht S, Feldmann G, Koorstra JB, Mullendore M, Alvarez H, et al. (2008) In vivo characterization of a polymeric nanoparticle platform with potential oral drug delivery capabilities. *Mol Cancer Ther* 7: 3878-3888.
- Duncan R, Izzo L (2005) Dendrimer biocompatibility and toxicity. *Adv Drug Deliv Rev* 57: 2215-2237.
- Langereis S, de Lussanet QG, van Genderen MHP, Backes WH, Meijer EW (2004) Multivalent contrast agents based on gadolinium-diethylenetriaminepentaacetic acid-terminated poly (propylene imine) dendrimers for magnetic resonance imaging. *Macromolecules* 37: 3084-3091.
- Hu HH, Nayak KS (2010) Change in the proton T(1) of fat and water in mixture. *Magn Reson Med* 63: 494-501.
- Rohrer M, Bauer H, Mintorovitch J, Requardt M, Weinmann H-J (2005) Comparison of magnetic properties of MRI contrast media solutions at different magnetic field strengths. *Investigative Radiology* 40: 715-724.
- Lasoroski A, Vuilleumier R, Pollet R (2013) Hyperfine interactions in a gadolinium-based MRI contrast agent: high-frequency modulations from ab initio simulations. *J Chem Phys* 139: 104115.
- Grant CW, Karlik S, Florio E (1989) A liposomal MRI contrast agent: phosphatidylethanolamine-DTPA. *Magn Reson Med* 11: 236-243.
- Grant CW, Barber KR, Florio E, Karlik S (1987) A phospholipid spin label used as a liposome-associated MRI contrast agent. *Magn Reson Med* 5: 371-376.
- Lu J, Ma S, Sun J, Xia C, Liu C, et al. (2009) Manganese ferrite nanoparticle micellar nanocomposites as MRI contrast agent for liver imaging. *Biomaterials* 30: 2919-2928.
- Kessinger CW, Khemtong C, Togao O, Takahashi M, Sumer BD, et al. (2010) In vivo angiogenesis imaging of solid tumors by alpha(v)beta(3)-targeted, dual-modality micellar nanoprobe. *Exp Biol Med (Maywood)* 235: 957-965.